ELSEVIER

Catalysis Today 55 (2000) 269–280

CATALYSIS TODAY

www.elsevier.com/locate/cattod

Comparison of alumina-, silica-, titania-, and zirconia-supported $FePO_4$ catalysts for selective methane oxidation

R.L. McCormick *, G.O. Alptekin

Department of Chemical Engineering and Petroleum Refining, Colorado School of Mines, Golden, CO 80401–1887, USA

Abstract

$FePO_4$ catalysts supported on Al_2O_3, ZrO_2, TiO_2 and SiO_2 and with iron loading from 2 to 16 wt% were tested in selective oxidation of methane, using molecular oxygen, in a continuous-flow reactor, at atmospheric pressure. The main products of the reaction were HCHO, CO and CO_2. For the silica-supported catalysts, small but quantifiable amounts of CH_3OH were also identified. Catalytic activity and selectivity exhibited a clear dependence on the oxide support and on $FePO_4$ loading. $FePO_4$ on silica produced the highest yield of the desired oxygenates, while alumina-supported $FePO_4$ exhibited the lowest selectivity to formaldehyde. The highest selectivity and space–time yield to formaldehyde and methanol were observed at lower $FePO_4$ loading levels for the SiO_2, ZrO_2, and TiO_2 supports. Loading had no effect on yield for $FePO_4$ supported on alumina. Mössbauer spectra suggest that when $FePO_4$ is supported on silica or zirconia, Fe species in fivefold coordination are formed. XPS results indicate a lower surface oxidation state for Fe on the silica support, and a substantial enrichment of the surface in phosphorus relative to less selective catalysts. The presence of easily reducible iron, in high coordination and isolated by phosphate groups is proposed to be responsible for the superior performance of the silica-supported $FePO_4$ catalyst. Stability of the desired products on the support also plays an important role in achieving a high yield.

1. Introduction

In the oxidation of hydrocarbons, supported metal oxide catalysts exhibit different activity and selectivity to the desired oxygenated hydrocarbon products, depending on the support material [1–4]. Higher activity and selectivity to the desired products over supported catalysts, as compared to bulk oxides, can, in part, be attributed to the formation of easily reducible supported metal oxide phases [5–8]. The nature of the metal oxide–support interaction has been widely investigated for MoO_3 and V_2O_5-based catalysts supported on conventional oxides (Al_2O_3, SiO_2, TiO_2, etc.). In these studies, it is shown that metal oxide–support interaction controls both, the reducibility and dispersion of the active phase [1,7], and in some cases leads to dramatic enhancement in catalytic activity and selectivity relative to unsupported oxides.

Among the different support materials, silica appears to be the most effective for selective oxidation of methane to formaldehyde [4,9–11]. Production of oxidation products over the silica support itself has also been documented [12]. Some authors propose that the supported metal oxide phase is not the active catalyst in these systems, but modifies or promotes the activity of the silica support [13,14]. A variety of metal ions have been investigated as additives on silica, and promoting as well as poisoning effects of these additives have been reported [8,15]. The role attributed to these promoters is to provide redox centers, which acceler-

* Corresponding author. Tel.: +1-303-273-3967; fax: +1-303-273-3730.
E-mail address: rlmccorm@mines.edu (R.L. McCormick).

0920-5861/00/$ – see front matter
PII: S0920-5861(99)00243-6

ate the activation of oxygen. This enhances the activity of silica, which exhibits high selectivity but poor catalytic activity for formaldehyde formation.

Other supports, such as Al_2O_3 and TiO_2, have also been studied, particularly for vanadia. However, poor performance towards formaldehyde formation has been reported to date [6,16]. Zirconium oxide as a support for metal oxide catalysts in methane oxidation has not been investigated in detail. Otsuka and Hatano [17] reported that ZrO_2 does not catalyze methane conversion to formaldehyde.

We have recently shown that silica supported $FePO_4$ exhibits relatively high activity and selectivity for oxidation of methane to methanol and formaldehyde [18]. In comparison to unsupported $FePO_4$, formaldehyde yield was nearly one order of magnitude higher. Also, methanol is not observed as a reaction product over the unsupported catalyst. The formation of an easily reducible iron site, containing iron in fivefold coordination and isolated by surface phosphate groups, was proposed to be responsible for the formation of partial oxidation products in high yield. In the present contribution, a series of $FePO_4$ catalysts on different oxide supports (alumina, zirconia, titania and silica) were examined for the methane partial oxidation reaction in order to determine the most effective support and to learn more about the iron phosphate–support interaction. These catalyst preparations were characterized by surface and bulk analysis techniques to provide insight into the impact of different support materials on structure of the iron phosphate phase.

2. Experimental setup and procedures

2.1. Catalyst preparation

The supported $FePO_4$ catalysts were prepared by impregnation of alumina (Alfa Aesar, 182 m^2/g), titania (Degussa, 61 m^2/g), zirconia (Degussa, 47 m^2/g) or 'precipitated' acid-washed silica (Cerac Chemicals, 398 m^2/g) with aqueous solutions of ferric nitrate and ortho-phosphoric acid. Prior to impregnation, the supports were dried at 673 K in air. For each material, the iron nitrate solution of concentration that ensured the desired iron loading was added to the dried support first. This material was dried overnight to give a free-flowing powder, to which was then added a stoichiometric ortho-phosphoric acid solution to provide a P/Fe ratio of unity. Impregnation was followed by evaporation at 363 K with continuous stirring, and calcining in air for 24 h at 973 K. Catalysts with $FePO_4$ loading of 2, 4 and 16 wt% were prepared (as well as 8 wt% for silica). All catalysts were compressed at 20 000 kPa and, subsequently, crushed and sieved to obtain pellets of 0.2–0.3 mm particle size range.

2.2. Catalyst characterization

Specific surface areas of the catalyst samples were measured using a Micromeretics Accusorb 2100E instrument. Nitrogen was used as adsorbate at liquid nitrogen temperature. X-ray powder diffraction (XRD) patterns were obtained using a Rigaku diffractometer with Cu $K\alpha$ radiation ($\lambda = 1.5432$ Å). A Kratos Electronics spectrometer with monochromatic Al $K\alpha$ radiation was used to obtain X-ray photoelectron spectra (XPS). The binding energy of C 1*s* (284.6 eV) was used as a reference in these measurements. The surface stoichiometry (P/Fe) was determined using the integrated peak intensities of the Fe $2p_{3/2}$ and P 2*p* signals, Scofield photoionization cross sections, and the classical relationship given by Scofield [19]. Coulston has discussed the difficulties inherent in determining surface stoichiometry for transition metal oxides and phosphates [20], and shown that, for vanadium phosphates, procedures similar to those employed here significantly overestimate the surface phosphorus-to-metal ratio. This difficulty can be overcome by the use of a suitable set of calibration standards; however, such a calibration has not yet been performed for the iron–phosphorus system. Therefore, the actual values of surface P : Fe reported should be regarded with suspicion. Comparison of P : Fe values between catalysts in order to examine directional trends should remain valid. Mössbauer spectra were recorded at room temperature, using a 25 m ^{57}Co/Rh source and a conventional constant acceleration spectrometer, operated in a triangular mode. Data acquisition was performed with standard multi-channel scaling and data analysis by the least squares fit of Lorentzian components. By computer folding and fitting, isomer shifts (δ) with respect to α-Fe, quadrupole splittings (Δ) and the line widths (Γ)

were calculated with a precision of ca. 0.01 mm s^{-1}. The accuracy for hyperfine field (H) determinations was 0.2 kOe. The samples were diluted in powdered sugar to avoid excessive Mössbauer absorption, and pressed into pellets.

2.3. Catalyst testing

Steady-state reactor studies were performed in fixed-bed micro-reactor in a manner identical to that employed in previous studies [21]. The reactor was a quartz tube, 30 cm long with 0.9 cm i.d. at the catalyst bed portion, mounted vertically in a tubular furnace. Typically, ca. 0.1 g of silica- or alumina-supported $FePO_4$ or 0.15 g of zirconia- or titania-supported $FePO_4$ was loaded into the reactor and covered with 15-mm layer of quartz beads to obtain a preheating zone and uniform gas distribution. Prior to reaction, the catalyst was calcined in situ under helium flow (20 ml/min) at the reaction temperature for about two hours. Methane conversion was below 10% for most experiments reported. Overall carbon balance closures obtained were within ±5%, and mostly within ±3%. Fractional conversion and product selectivity were defined as:

$$\text{Conversion} = \frac{\text{moles (HCHO + CO + CO}_2\text{) formed}}{\text{moles of CH}_4\text{ fed}} \quad (1)$$

$$\text{Selectivity} = \frac{\text{moles of HCHO formed}}{\text{moles (HCHO + CO + CO}_2\text{) formed}} \quad (2)$$

An on-line Hewlett–Packard 5890 gas chromatograph (GC), equipped with a thermal conductivity detector, was used to analyze reactant and product streams. GC system and calibration techniques have been described in detail previously [21].

3. Results

3.1. Catalyst characterization

BET surface areas and calculated surface density (formula unit per nm^2) of $FePO_4$ in the supported catalyst samples are presented in Table 1. BET surface areas of the titania- and zirconia-supported catalysts did not change appreciably upon impregnation of $FePO_4$ at low loadings. However, the silica- and alumina-supported $FePO_4$ samples exhibited a significantly lower surface area than the bare supports. This decline in surface area can be explained by blocking of micro-pores of silica and alumina with the deposited iron phosphate phase.

Table 1
BET surface area and surface density of the alumina-, zirconia-, titania- and silica-supported $FePO_4$ catalysts

Catalyst	$FePO_4$ loading (%)	Surface area (m^2/g)	Surface density (molecule/nm^2)
Al_2O_3	–	182	–
$FePO_4/Al_2O_3$	2	146	0.53
	4	127	1.22
	16	101	6.15
ZrO_2	–	47	–
$FePO_4/ZrO_2$	2	41	1.89
	4	31	5.01
	16	24	25.9
TiO_2	–	61	–
$FePO_4/ZrO_2$	2	52	1.50
	4	49	3.17
	16	30	20.7
$FePO_4/SiO_2$	2	288	0.27
	4	226	0.69
	8	171	1.82
	16	104	5.98

XRD patterns of the alumina-, zirconia-, and titania-supported $FePO_4$ samples with 2, 4 and 16 wt% are presented in Figs. 1–3, respectively. Diffraction peaks of aluminum oxide (gamma), zirconium oxide, and titanium oxide are evident. No peaks corresponding to crystalline $FePO_4$ or other iron phosphate phases were detected at the 2 and 4 wt% loading levels. It can be concluded that the loading of the active phase is so low, or iron phosphate is so highly dispersed, that no pattern can be detected. At 16 wt% $FePO_4$, diffraction peaks of the quartz form of $FePO_4$ are evident, indicating the formation of crystalline iron phosphate. XRD pattern of silica-supported $FePO_4$ [22], on the other hand, exhibited peaks at 20.1° and 25.8°, characteristic of the quartz form of $FePO_4$ [23], even for the lowest loading level.

Mössbauer spectroscopy was used to determine the chemical state and coordination of iron species in these samples. Hyperfine interaction parameters

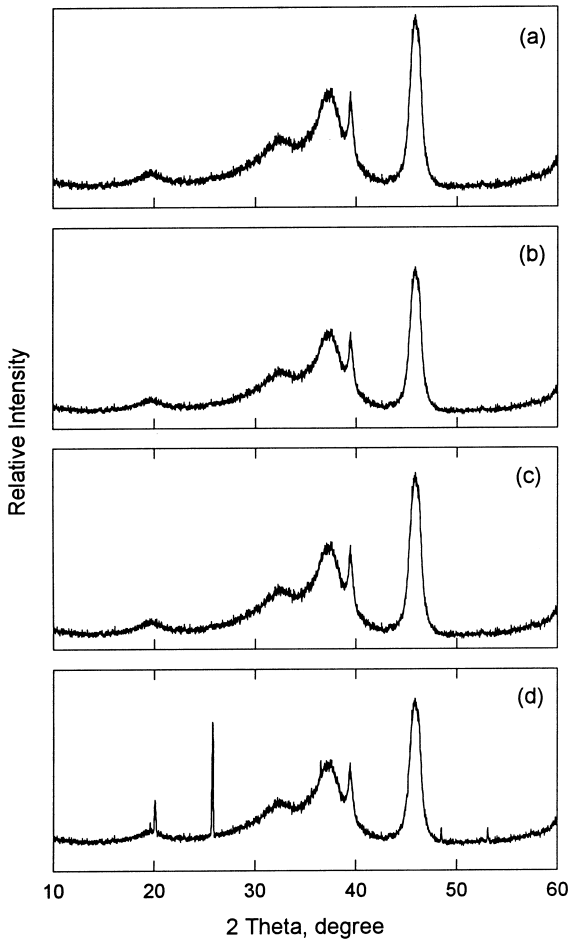

Fig. 1. XRD patterns of the (a) Al_2O_3; (b) 2 wt% $FePO_4/Al_2O_3$; (c) 4 wt% $FePO_4/Al_2O_3$; and (d) 16 wt% $FePO_4/Al_2O_3$ catalysts.

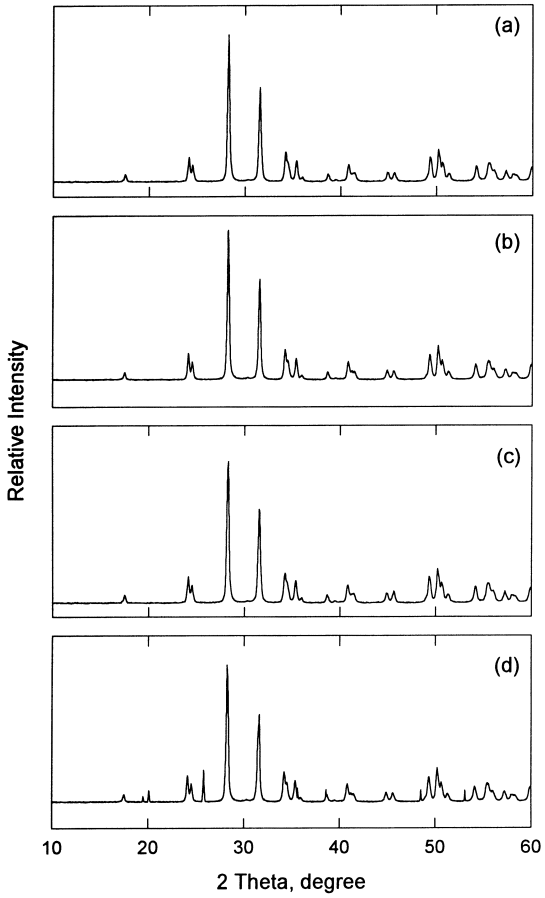

Fig. 2. XRD patterns of the (a) ZrO_2; (b) 2 wt% $FePO_4/ZrO_2$; (c) 4 wt% $FePO_4/ZrO_2$; and (d) 16 wt% $FePO_4/ZrO_2$ catalysts.

(along with those of bulk $FePO_4$ for comparison) are listed in Table 2. Except for silica, the best fit of the spectra was obtained with a single doublet. The best fit for silica-supported $FePO_4$ was obtained with two doublets, indicating iron in two different chemical environments. For the alumina-, zirconia- and titania-supported $FePO_4$ samples, hyperfine interaction parameters exhibit similar trends. At the 16 wt% loading level, isomer shift (δ) and quadrupole splitting (Δ) take values similar to those of bulk $FePO_4$, i.e. $\delta = 0.28\,\text{mm s}^{-1}$, and $\Delta = 0.64\,\text{mm s}^{-1}$. As the loading level goes down, isomer shift increases, which may be attributed to an increase in the electron density of the iron sites. The highest shift was observed for the 2 wt% $FePO_4/ZrO_2$ sample with $\Delta = 1.08\,\text{mm s}^{-1}$, the titania-supported samples exhibited a smaller increase to a value of $\Delta = 0.81\,\text{mm s}^{-1}$, while almost no change is evident for the alumina-supported catalysts. A significantly higher quadrupole splitting than that of bulk $FePO_4$ was observed for the 2 and 4 wt% loading levels for all samples. This may be an indication of higher coordination of Fe compared to the tetrahedral environment of $FePO_4$, and is consistent with the formation of a strongly interacting, X-ray amorphous phase.

In the silica-supported $FePO_4$ samples, iron is present in two different chemical environments. Component 1 is clearly similar to bulk $FePO_4$ and must correspond to the $FePO_4$ phase observed by X-ray diffraction. The fraction of iron present in Component 1 increases with increasing loading. The Mössbauer

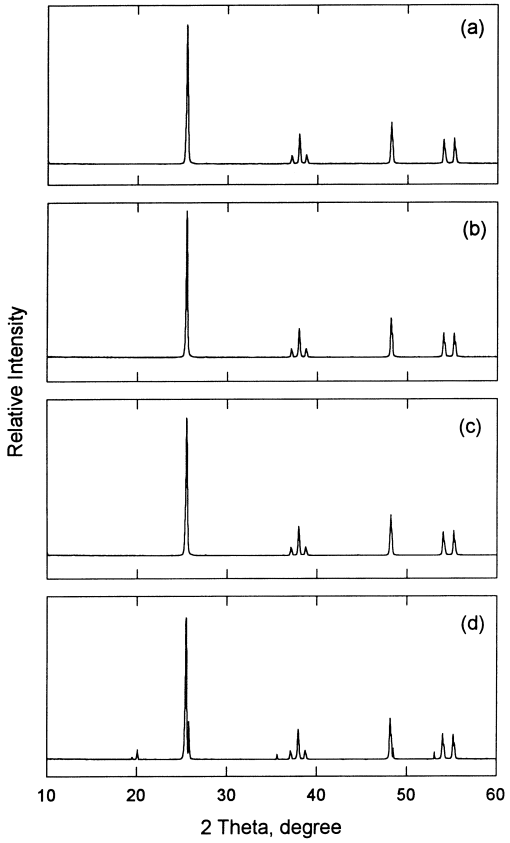

Fig. 3. XRD patterns of the (a) TiO_2; (b) 2 wt% $FePO_4/TiO_2$; (c) 4 wt% $FePO_4/TiO_2$; and (d) 16 wt% $FePO_4/TiO_2$ catalysts.

isomer shift and quadrupolar splitting values for Component 2 are similar to those observed at low loading on the other supports. Thus, this X-ray amorphous phase contains Fe in higher coordination than in bulk $FePO_4$. The increase in the isomer shift is even larger than observed for ZrO_2 and suggests a decrease in the effective oxidation state. The quadrupole splitting of this component is typical of fivefold coordinate Fe, as reported for ferric oxyphosphate or $Fe_3(PO_4)O_3$, by De Guire et al. [24]. That Fe in ferric oxyphosphate is present in fivefold coordination (trigonal bipyramid) was shown in X-ray diffraction studies [25]. Interaction of $FePO_4$ with all of the supports apparently produces Fe in a similar coordination environment.

XPS Fe $2p_{3/2}$ binding energies and the surface atomic P/Fe ratio for the supported $FePO_4$ catalysts with 2 wt% loading are presented in Table 3. Binding energy of the Fe $2p_{3/2}$ transition changed noticeably for the supported samples. A 1.2-eV shift to lower binding energy, relative to bulk $FePO_4$, occurs for the $FePO_4/SiO_2$ catalyst. For the $FePO_4$ samples supported on alumina, titania and zirconia, a smaller decrease of 0.3, 0.8 and 1.0 eV, respectively, was observed. The decrease in the binding energy is attributed to a change in the surface oxidation state of iron. These results indicate that the weakest electronic interaction between the support and supported $FePO_4$ phase occurs for the alumina-supported sample. The surface P/Fe atomic ratio was significantly higher for the silica- and zirconia-supported samples than for the other preparations. For the alumina-supported sample, P : Fe was ≈1.0, although, given uncertainties in calibration of this analytical method, it is not known if this indicates a stoichiometry identical to that of bulk $FePO_4$. A significant deficiency of surface phosphorus, relative to the other samples, was evident for the titania-supported catalyst.

3.2. Steady-state reactor studies

The results of comparative tests of the oxide supports themselves are summarized in Table 4. With ZrO_2, formation of slight amounts of coupling products has been reported in some cases [13], but, under the conditions employed in this study, formation of the higher-order products was not observed. Only carbon oxides were detected for ZrO_2, as well as for the Al_2O_3 and TiO_2 supports. Silica exhibited a significant selectivity to formaldehyde, in agreement with previous reports [16].

The products of methane oxidation over the 2 wt% $FePO_4$ on alumina, titania, zirconia and silica catalysts are carbon monoxide, carbon dioxide and formaldehyde, and for silica, methanol. Selectivity to these products is presented in Figs. 4–7 as a function of methane conversion, varied by varying gas hourly space velocity (GHSV), at a methane-to-oxygen ratio of 1.0. For all catalysts, selectivity to formaldehyde is maximized at methane conversion approaching zero, suggesting that formaldehyde is a primary product. As methane conversion increases, selectivity to formaldehyde decreases rapidly. For the silica-supported material at this loading, selectivity to CO approaches zero at 0% conversion, suggesting a predominantly sequential reaction path. For the other catalysts, methane is apparently converted to CO and

Table 2
Hyperfine interaction parameters of alumina-, zirconia- and titania-supported $FePO_4$ catalysts

Catalyst	Loading (wt%)	Susceptible components	δ (mm/s)	Δ (mm/s)	Γ (mm/s)	Relative intensity (%)
$FePO_4/Al_2O_3$	2	1	0.31 (1)[a]	1.00 (1)	0.64 (2)	100
	4	1	0.30 (1)	0.99 (3)	0.62 (1)	100
	16	1	0.27 (1)	0.63 (1)	0.27 (1)	100
$FePO_4/ZrO_2$	2	1	0.34 (1)	1.08 (3)	0.53 (4)	100
	4	1	0.33 (1)	1.04 (4)	0.51 (5)	100
	16	1	0.28 (1)	0.62 (1)	0.25 (2)	100
$FePO_4/TiO_2$	2	1	0.33 (1)	0.81 (1)	0.49 (3)	100
	4	1	0.32 (2)	0.81 (2)	0.49 (3)	100
	16	1	0.29 (1)	0.63 (2)	0.26 (1)	100
$FePO_4/SiO_2$	2	1	0.31 (1)	0.59 (2)	0.34 (2)	42
		2	0.35 (1)	1.06 (3)	0.44 (2)	58
	4	1	0.30 (1)	0.61 (1)	0.33 (2)	80
		2	0.38 (3)	0.96 (9)	0.35 (6)	20
	8	1	0.31 (1)	0.61 (3)	0.38 (2)	88
		2	0.35 (2)	1.04 (5)	0.26 (12)	12
	16	1	0.28 (1)	0.65 (1)	0.30 (1)	51
		3	0.50 (1)	0.57 (1)	0.43 (2)	49
$FePO_4$ bulk	–	1	0.28 (1)	0.64 (1)	0.31 (1)	100

[a] The values within parentheses represent the experimental uncertainty.

HCHO in parallel. It is unclear whether methanol formation over the silica-supported catalyst occurs as the first step in a sequence or in parallel with other paths. Alumina-supported $FePO_4$ exhibited a very high activity at 873 K. In order to collect data under differential reactor conditions, experiments for alumina-supported catalysts were performed at 773 K. Even at a 100 K lower temperature, 2 wt% $FePO_4/Al_2O_3$ was observed to be very active and yielded the lowest selectivity to formaldehyde. Silica-supported $FePO_4$ exhibited the best performance in catalyzing the formation of the partial oxidation products, methanol and formaldehyde. Zirconia- and titania-supported $FePO_4$ catalysts exhibited moderate selectivity to formaldehyde, and an appreciable activity in oxidizing methane despite their low surface areas.

Temperature dependence of the methane oxidation rate was determined by varying the temperature between 773 and 923 K. The reaction orders in methane and oxygen over silica-supported $FePO_4$ (5 wt%), were previously reported to be 0.61 ± 0.07 and 0.28 ± 0.03, respectively [18]. These reaction orders were used for the calculation of rate constants and Arrhenius parameters. Activation energies in the range of 103 ± 9 to 167 ± 9 kJ/mol were observed for iron phosphate on different supports, as reported in Table 5 . Previously, an activation energy of 174 ± 9 kJ/mol was reported for methane oxidation over bulk $FePO_4$ [18]. For the 2 wt% $FePO_4$ loaded samples, supporting $FePO_4$ on silica did not cause a significant change in the global activation energy for methane oxidation. However, all other supports exhibit significantly lower activation energy, with $FePO_4$ on alumina yielding the lowest value.

Table 3
XPS binding energies and surface atomic P/Fe ratio for alumina-, zirconia- and titania-supported $FePO_4$ (2 wt%) catalysts

Catalyst	Fe $2p_{3/2}$ (eV)[a]	P/Fe
$FePO_4/Al_2O_3$ (2 wt%)	712.2 (3.9)[b]	1.03
$FePO_4/ZrO_2$ (2 wt%)	711.5 (4.0)	1.62
$FePO_4/TiO_2$ (2 wt%)	711.7 (5.2)	0.52
$FePO_4/SiO_2$ (2 wt%)	711.3 (3.9)	2.17
Bulk $FePO_4$	712.5 (3.7)	0.92

[a] Binding energies are reliable within ± 0.3 eV.
[b] The values within parentheses indicate full width at half maximum (FWHM) values.

Significant difference in the surface areas of the supports used in this study requires comparison using parameters eliminating the influence of the surface area. The specific surface activity (SAA, nmol

Table 4
Activity and selectivity of the various oxide supports in methane partial oxidation reaction

Catalyst	Surface area (m^2/g)	Temperature (K)	Rate (10^{-6} mol/s g)	Selectivity (%)			
				C_2	HCHO	CO	CO_2
Al_2O_3	182	773	10.9[a]	–	–	34	66
ZrO_2	47	873	0.89	–	–	29	71
TiO_2	61	873	1.07	–	–	68	32
SiO_2-ppt.	388	873	0.49	–	63	14	23

[a] See text for reaction conditions.

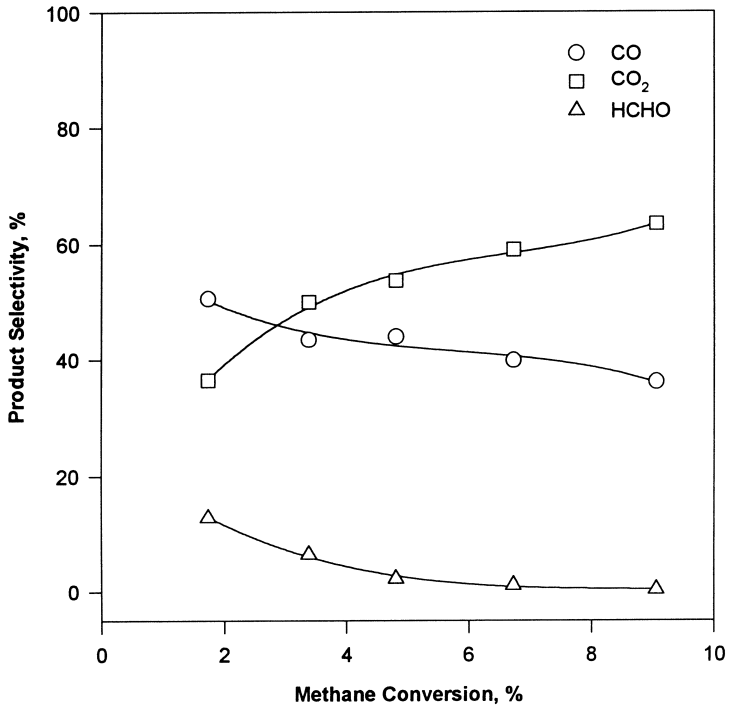

Fig. 4. Product selectivity as function of methane conversion over alumina-supported $FePO_4$ (2 wt%). $P_{CH_4} = 49$ kPa; $P_{O_2} = 48$ kPa; GHSV = 20 000–70 000 h^{-1}; and $T = 773$ K.

$CH_4\ s^{-1}\ m^{-2}$) and surface productivity of formaldehyde (SP_{HCHO} nmol $m^{-2}\ s^{-2}$) were calculated for the different $FePO_4$ preparations and are listed in Table 5. Among these catalysts, zirconia-supported $FePO_4$ exhibits the highest SSA and SP. Titania-supported $FePO_4$ is just as active on this basis, but exhibits a much lower selectivity. However, because of the much higher surface area and higher HCHO selectivity, silica-supported catalysts produce the highest space–time yields as reported in Table 6.

The effect of $FePO_4$ loading on the alumina-, zirconia-, titania- and silica-supports was also examined. The results of these experiments are summarized in Table 6. The highest selectivity and space–time yield (STY) to formaldehyde and methanol were obtained with the lower $FePO_4$ loading levels for the silica-supported catalysts. The maximum STY of formaldehyde and methanol were 622 g/kg_{cat} h at 973 K and 25 g/kg_{cat} h at 873 K (GHSV of 62 500 h^{-1}; note that these conditions are different from those of Table 6). Yields towards the desired products decreased significantly by increasing the iron content. Similar trends, though not as profound, were observed for zirconia-supported $FePO_4$. For Al_2O_3- and TiO_2-supported catalysts, $FePO_4$ loading did not significantly effect the product distribution .

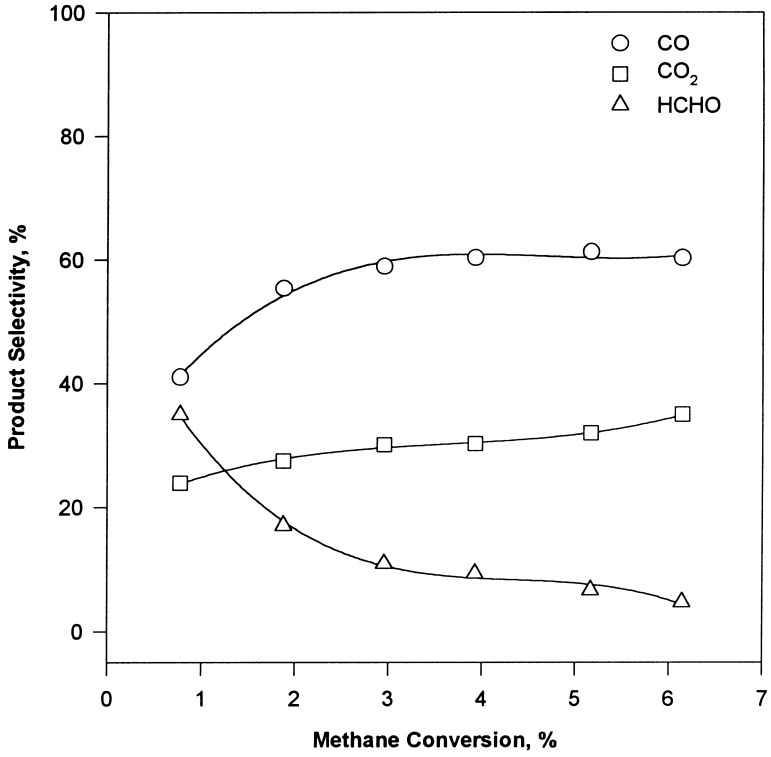

Fig. 5. Product selectivity as function of methane conversion over zirconia-supported $FePO_4$ (2 wt%). $P_{CH_4} = 49$ kPa; $P_{O_2} = 48$ kPa; GHSV = 20 000–70 000 h^{-1}; and $T = 873$ K.

Table 5
Kinetic parameters and surface productivity of formaldehyde over the alumina-, zirconia-, titania- and silica-supported $FePO_4$ (2 wt%) catalysts

Catalyst	Reaction rate[a] (mol/g_{cat} s)	Activation energy (kJ/mol)	Pre-exponential factor (mol/g_{cat} s $kPa^{0.89}$)	SSA[b] ($nmol_{CH_4}$ m^{-2} s^{-1})	SP HCHO[c] (nmol m^{-2} s^{-1})
$FePO_4/Al_2O_3$[d]	1.6×10^{-6}	103 ± 9	6.1×10^{1}	10.9	1.10
$FePO_4/ZrO_2$	1.3×10^{-6}	143 ± 6	6.2×10^{3}	32.4	23.7
$FePO_4/TiO_2$	1.7×10^{-6}	153 ± 6	2.4×10^{4}	33.0	8.81
$FePO_4/SiO_2$	0.6×10^{-6}	167 ± 9	7.3×10^{4}	2.17	19.1

[a] $T = 873$ K; $F_{CH_4} = 2.3 \times 10^{-3}$ mol/min; $CH_4 : O_2 = 1$; W_{cat} 0.1 g $FePO_4/SiO_2$; 0.15 g $FePO_4/ZrO_2$ and $FePO_4/TiO_2$.
[b] Specific surface activity.
[c] Surface productivity of HCHO.
[d] $T = 773$ K; $F_{CH_4} = 2.3 \times 10^{-3}$ mol/min; $CH_4 : O_2 = 1$; W_{cat} 0.1 g $FePO_4/Al_2O_3$.

4. Discussion

The catalytic activity and selectivity of iron phosphate was significantly influenced by choice of support for the methane partial oxidation reaction. The space–time yield to the desired oxygenated products was used to rank the performance of these $FePO_4$ preparations. Based upon this criteria, silica-supported $FePO_4$ was determined to be the best catalyst (622 g/kg_{cat} h), while alumina-supported $FePO_4$ exhibited the lowest formaldehyde yield (15–20 g/kg_{cat} h). Formation of observable quantities

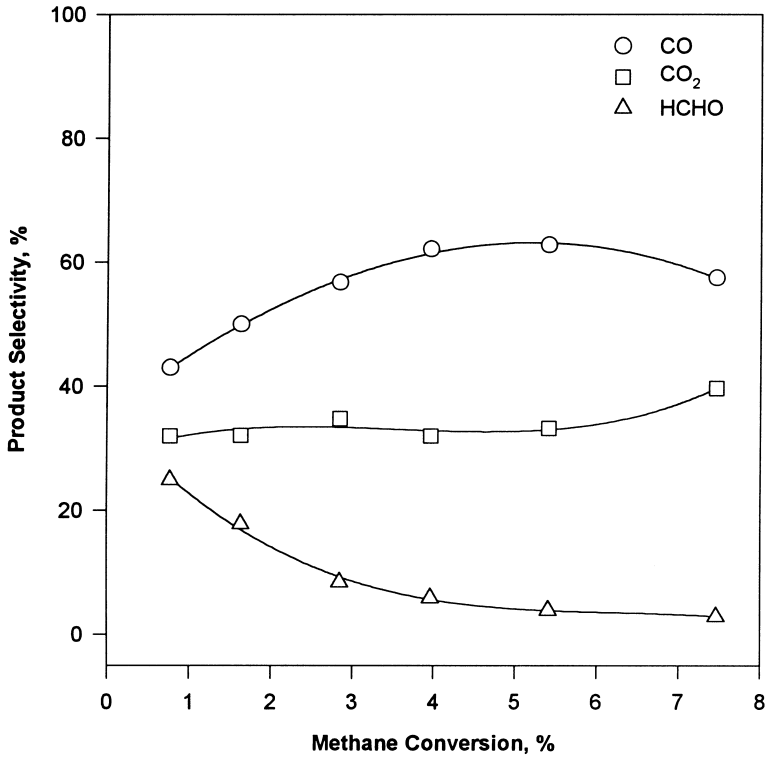

Fig. 6. Product selectivity as function of methane conversion over titania-supported $FePO_4$ (2 wt%). $P_{CH_4} = 49$ kPa; $P_{O_2} = 48$ kPa; GHSV = 20 000–70 000 h^{-1}; and $T = 873$ K.

Table 6
Effect of $FePO_4$ loading on the catalytic activity over alumina, zirconia, titania and silica supports[a]

Catalyst	Loading (wt.%)	CH_4 conversiom (%)	Selectiviy (%)				STY (g/kg_{cat}-h)	
			CH_3OH	HCHO	CO	CO_2	CH_3OH	HCHO
$FePO_4/Al_2O_3$[b]	2	4.1	–	1	44	55	–	17
	4	4.6	–	1	41	58	–	19
	16	3.9	–	1	46	53	–	17
$FePO_4/ZrO_2$	2	3.4	–	11	60	29	–	105
	4	3.9	–	7	55	37	–	77
	16	3.6	–	6	53	38	–	61
$FePO_4/TiO_2$	2	4.4	–	4	62	34	–	49
	4	4.8	–	3	58	39	–	40
	16	3.8	–	2	54	44	–	21
$FePO_4/SiO_2$	2	1.6	2	88	9	<1	15	593
	4	1.7	1	69	25	5	7	494
	16	2.1	–	34	54	12	–	301

[a] $T = 873$ K; $F_{CH_4} = 2.3 \times 10^{-3}$ mol/min; $CH_4 : O_2 = 1$, W_{cat} 0.1 g $FePO_4/SiO_2$; 0.15 g $FePO_4/ZrO_2$ and $FePO_4/TiO_2$.
[b] $T = 773$ K; $F_{CH_4} = 2.3 \times 10^{-3}$ mol/min; $CH_4 : O_2 = 1$; W_{cat} 0.1 g $FePO_4/Al_2O_3$.

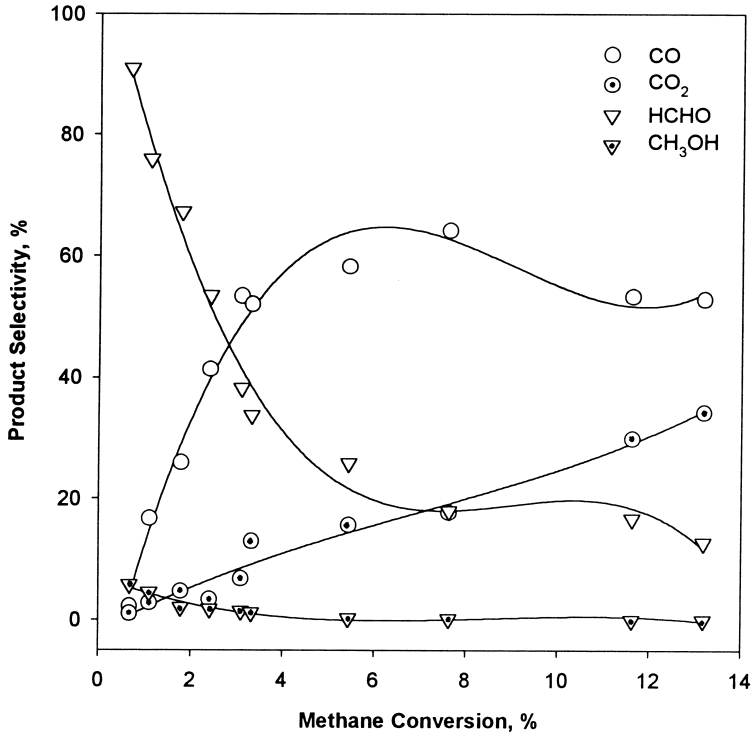

Fig. 7. Product selectivity as function of methane conversion over silica-supported $FePO_4$ (2 wt%). $P_{CH_4} = 49.5$ kPa; $P_{O_2} = 49.5$ kPa; GHSV = 10 000–60 000 h^{-1}; and $T = 873$ and 928 K.

of methanol was only observed for the silica-supported catalyst. We have previously reported formaldehyde space–time yield up to 60 g/kg_{cat} h over bulk $FePO_4$ [18]. Supporting $FePO_4$ on aluminum oxide led to a large increase in the catalytic activity; however, the selectivity to formaldehyde severely decreased. Kinetic studies revealed a significantly lower activation energy for methane oxidation over alumina-supported $FePO_4$, than for the other catalysts. The surface acidity of alumina may promote easy activation of methane. Cheng [26] has investigated the stability of formaldehyde over several oxides, and SiO_2 was observed to be relatively inert for formaldehyde oxidation. Al_2O_3 and TiO_2 were found to be very active, perhaps also because of the acid properties of these materials. Thus, low yield over catalysts on these supports can be attributed to participation of the support in further oxidation of formaldehyde. $FePO_4$ on zirconia produced slightly higher formaldehyde yield than the titania-supported material, but much less than silica. However, when viewed on a surface productivity basis (nmol of HCHO/m^2 s, reported in Table 5), $FePO_4/ZrO_2$ exhibited an even higher productivity than $FePO_4/SiO_2$. The zirconia-supported catalyst is more active per unit mass and has a much lower surface area than the silica-supported catalyst; space–time yield is lower because actual formaldehyde space–time yield is lower as the selectivity over $FePO_4/ZrO_2$ is lower.

The catalytic activity and selectivity to formaldehyde was effected by the $FePO_4$ content for the silica and zirconia-supported catalysts, and to a lesser extent for the titania-supported material. It is evident that the increase in selectivity to formaldehyde with decreasing loading is primarily because of decreased rates of formation of CO and CO_2. The negative influence of the iron phosphate loading on formaldehyde selectivity may be a consequence of re-adsorption of formaldehyde, and the presence of surface structures promoting formation of total oxidation products. In particular, bulk $FePO_4$ exhibits conversion of methane to CO_2 and HCHO in parallel [18], and

low HCHO yield over the 16% loaded catalysts may, therefore, reflect extensive formation of $FePO_4$ crystallites. A highly dispersed form of iron phosphate, which is structurally different from $FePO_4$ as discussed below, apparently does not catalyze the direct conversion of methane to CO_2. For the alumina- and titania-supported $FePO_4$ samples, loading level caused only a very slight change in the selectivity to formaldehyde. Furthermore, at the highest $FePO_4$ loading level (16 wt%), the catalytic activity of these materials declined substantially. This decline may be explained by the fact that at high loading, highly active exposed Al_2O_3 and TiO_2 sites are covered with less active $FePO_4$.

X-ray diffraction results show the presence of crystalline $FePO_4$ at all loading levels for the silica-supported catalysts, but do not indicate crystalline $FePO_4$ for the other supports at loadings <16 wt%. Mössbauer spectra of the silica supported samples also show $FePO_4$ but also indicate the presence of a second iron containing component. Based on hyperfine interaction parameters this second component contains iron in a higher coordination environment than $FePO_4$ and with a higher electron density. As noted above, the quadrupole splitting is typical of iron in fivefold coordination, similar to the coordination environment of iron oxyphosphate, $Fe_3(PO_4)O_3$ [21] . For the zirconia-supported $FePO_4$, the second best catalyst, hyperfine interaction parameters are similar to those of the fivefold coordinate phase observed for the silica support. The presence of iron in a higher coordination (most likely a fivefold) relative to $FePO_4$ apparently promotes the formation of selective products. For the alumina- and titania-supported catalysts, although the quadrupole splitting value is higher than that of bulk $FePO_4$, no significant changes were observed in the isomer shift. Isomer shift is an important indicator of the electron density on Fe sites. As loading is increased to 16%, the Mössbauer parameters for all catalysts become similar to those for bulk $FePO_4$. X-ray photoelectron spectra confirm the conclusion of higher electron density on iron in the silica-supported catalyst as binding energy is reduced by 1.2 eV relative to crystalline $FePO_4$. The binding energy shift is roughly 1 eV for zirconia and titania and is probably negligible for alumina. XPS also shows that the most selective catalysts (supported on SiO_2 or ZrO_2) exhibit surface P/Fe ratios in excess of those observed for bulk $FePO_4$ and for the less selective supported catalysts.

Comparison of catalyst activity and yield with the characterization results suggests that the highest yields are obtained over catalysts containing iron in high coordination (fivefold vs. fourfold), with a higher electron density (lower effective oxidation state), and with high surface P : Fe ratio. This suggests a mechanistic picture where, under reaction conditions, the fivefold coordinate reduced iron provides a site for chemisorption of a reactive oxygen species. This reactive oxygen species is then responsible for activation of methane [9,27]. The site is isolated by surface phosphate groups inhibiting over oxidation. The surface phosphate groups may also allow facile formation of surface hydroxyls and desorption of water [28,29], and may also be necessary for the formation of methanol [30,31].

Acknowledgements

The financial support for this work by the U.S. Department of Energy, Fossil Energy Branch under contract DE-AC22-PC92110 is gratefully acknowledged.

References

[1] G. Deo, I.E. Wachs, J. Catal. 129 (1991) 307.
[2] G. Deo, I.E. Wachs, J. Catal. 146 (1994) 323.
[3] I.E. Wachs, J.-M. Jehng, G. Deo, B.M. Weckhuysen, V.V. Guliants, J.B. Benziger, S. Sundaresan, J. Catal. 170 (1997) 75.
[4] A. Parmaliana, F. Arena, J. Catal. 167 (1997) 57.
[5] M.M. Koranne, J.C. Goodwin, G. Marcelin, J. Phys. Chem. 97 (1993) 673.
[6] M.M. Koranne, J.C. Goodwin, G. Marcelin, J. Catal. 148 (1994) 369.
[7] M.A. Banares, J.L.G. Fierro, J.B. Moffat, J. Catal. 142 (1993) 406.
[8] M.A. Banares, M. Alemany, M. Lopez-Granados, M. Faraldos, J.L.G. Fierro, Catal. Today 33 (1997) 73.
[9] F. Arena, N. Giordano, A. Parmaliana, J. Catal. 167 (1997) 66.
[10] S. Kasztelan, J.B. Moffat, Chem. Commun., 1987, 1663.
[11] Q. Sun, M. Jehng, H. Hu, R.G. Herman, I.E. Wachs, K. Klier, J. Catal. 165 (1997) 91.
[12] A. Parmaliana, F. Frusteri, A. Mezzapica, M.S. Scurrell, N. Giordiano, Chem. Commun., 1993, 751.
[13] A. Parmaliana, F. Frusteri, D. Miceli, A. Mezzapica, M.S. Scurrell, N. Giordano, App. Catal. 78 (1991) L7.

[14] A. Parmaliana, V. Sokolovskii, D. Micelli, F. Arena, N. Giordiano, J. Catal. 148 (1994) 514.
[15] T. Kobayashi, K. Nakagawa, K. Tabata, M. Haruta, Chem. Commun., 1994, 1609.
[16] A. Parmaliana, V. Sokolovskii, D. Miceli, F. Arena, N. Giordano, ACS Sypmp. Series 523 (1993) 43.
[17] K. Otsuka, M. Hatano, J. Catal. 108 (1987) 252.
[18] G.O. Alptekin, A.M. Herring, D.L. Williamson, T.R. Ohno, R.L. McCormick, J. Catal. 181 (1999) 104.
[19] J.H. Scofield, J. Electron Spectr. Relat. Phenom. 8 (1976) 129.
[20] G.W. Coulston, E.A. Thompson, N. Herron, J. Catal. 163 (1996) 122.
[21] R.L. McCormick, G.O. Alptekin, A.M. Herring, T.R. Ohno, S.F. Dec, J. Catal. 172 (1997) 160.
[22] G.O. Alptekin, D.L. Williamson, T.R. Ohno, R.L. McCormick, Topics in Catalysis, in press.
[23] E. Muneyama, A. Kunishige, K. Ohdan, M. Ai, J. Catal. 158 (1996) 378.
[24] M.R. DeGuire, T.R.S. Prasanna, G. Kalonji, R.C. O'Handley, J. Am. Ceram. Soc. 70 (1987) 831.
[25] A. Modaressi, A. Courtois, R. Gerardin, B. Malaman, C. Bleitzer, J. Sol. Stat. Chem. 47 (1983) 245.
[26] W.H. Cheng, J. Catal. 158 (1996) 477.
[27] A.W. Sexton, B. Kartheuser, C. Batiot, H.W. Zanthoff, B.K. Hodnett, Catal. Today 40 (1998) 245.
[28] J.R. Ebner, M.R. Thompson, Catal. Today 16 (1993) 51.
[29] P.A. Agaskar, L. DeCaul, R.K. Grasselli, Catal. Lett. 23 (1994) 339.
[30] R.S. Liu, K.Y. Liew, R.E. Johnson, J.H. Lunsford, J. Am. Chem. Soc. 106 (1984) 4117.
[31] S. Pak, C.E. Smith, M.P. Rosynek, J.H. Lunsford, J. Catal. 165 (1997) 73.